BILINGUAL PUBLISHING GROUP

Journal of Atmospheric Science Research

https://journals.bilpubgroup.com/index.php/jasr

ARTICLE

Spatial Changes of Driving Parameters Affecting Cyclonic Activity over the North Indian Ocean from 1960 to 2020

***Akshay Kumar Sagar , Arun Chakraborty* ***

Centre for Ocean, River, Atmosphere and Land Sciences (CORAL), Indian Institute of Technology Kharagpur, Kharagpur 221005, India

ABSTRACT

This study undertakes a thorough analysis of the elements that influence the variability of tropical cyclones (TC) in the North Indian Ocean (NIO) from 1960 to 2020, with a specific focus on the periods before and after the monsoon season. The study utilizes historical satellite data to investigate the factors that impact the formation, strength, and trajectories of cyclones. The primary method for evaluating cyclone strength is by calculating the Accumulated Cyclone Energy (ACE). The study observes a decreasing trend in ACE levels during 1991–2005, which started increasing just after from 2006 to 2020. The Bay of Bengal (BoB) has a more uniform distribution of ACE in comparison to the Arabian Sea (AS), with higher average values and more variability over the Main Development Region (MDR), which is the area where cyclone development occurs most frequently. Cyclones of greater intensity generally occur following the monsoon season. Examination of storm paths reveals that cyclones with greater intensity frequently hit the northeastern and southeastern coastal regions of India. The study emphasizes notable discrepancies in parameters within the MDR, which impact cyclone strength and ACE values throughout various periods.

Keywords: ACE; Tropical Cyclone; Bay of Bengal; Variability

*CORRESPONDING AUTHOR:

Arun Chakraborty, Centre for Ocean, River, Atmosphere and Land Sciences (CORAL), Indian Institute of Technology Kharagpur, Kharagpur 221005, India; Email: arunc@coral.iitkgp.ac.in

ARTICLE INFO

Received: 22 July 2024 | Revised: 28 August 2024 | Accepted: 10 October 2024 | Published Online: 15 October 2024

DOI: https://doi.org/10.30564/jasr.v7i4.6926

CITATION

Sagar, A.K., Chakraborty, A., 2024. Spatial Changes of Driving Parameters Affecting Cyclonic Activity over the North Indian Ocean from 1960 to 2020. Journal of Atmospheric Science Research. 7(4): 13–22. DOI: https://doi.org/10.30564/jasr.v7i4.6926

1. Introduction

The North Indian Ocean (NIO) is distinguished due to its unique thermodynamic conditions and intricate natural processes, encompassing two different basins: the Bay of Bengal (BoB) and the Arabian Sea (AS). Both locations are conducive to the production of tropical cyclones (TCs) due to many variables. These factors consist of elevated sea surface temperature (SST) beyond 26 °C, the Coriolis force, significant humidity, low vertical wind shear (VWS), and the presence of pre-existing weak low-pressure systems and upper-level divergence [1–4]. Tropical storms in the NIO mostly occur during two specific seasons: April–May, known as the pre-monsoon season, and October–November, known as the post-monsoon season. These cyclones have a considerable influence on the eastern coast of India, altering local climates and populations every year. According to historical statistics from the National Cyclone Risk Mitigation Project [5], the eastern coast witnessed over 308 cyclones between 1890 and 2000; whereas the western coast experienced only 48. In the study of cyclonic disturbances over five decades (1961–2010), where they observed that changes in translational speed increased as compared to the AS [6]. This suggests that cyclonic activity varies across these two basins and needs to be analyzed deeply on a smaller time scale. The frequency of TCs over the BoB (AS) has exhibited a decline (increase) over the recent three-decade period (1990–2019) in comparison to the past three decades (1960–1989) [7]. A decline in TC activity over BoB was noted in November, attributed to a notable reduction in mid-level relative humidity [8]. The findings of the study indicate a potential decline in the frequency of landfalling TCs in the region. However, there is a notable shift in the spatial distribution of landfalling TCs, with a heightened incidence of TCs occurring across northern India and Bangladesh. This shift may result in increased exposure to TC-related hazards in these regions [9].

A recent study emphasized the need to improve seasonal forecasting by extending the time frame to reduce the risks associated with cyclones more effectively [10]. They highlighted the necessity of being prepared and having a well-coordinated response to disasters. By contrast, the variations in the ability to identify cyclones among different maritime regions are also studied [11]. Climate variability variables, such as El-Niño, La-Niña, and local air pollution, have had a substantial impact on long-term tropical cyclone patterns since 1980 [12].

Although there have been improvements, there are still gaps in our understanding of the long-term variations in cyclone frequency, the variables that influence them, and the predictability of storm trajectories on a seasonal and monthly basis. Our research attempts to fill these gaps by examining certain characteristics and patterns of tropical cyclones from 1960 to 2020 during three unique periods. We chose the months of April and May as the pre-monsoon season and for the post-monsoon season, the months of October and November are selected and the parameters are further evaluated based on these periods. We first analyzed the variability of ACE and its spatial distribution over the NIO region to identify the regions most favorable to the cyclonic activity that affects ACE. Then, the tracks and landfall locations were examined based on different categories to check the frequency and intensity of TC events. We further studied the variations in parameters that influence cyclonic activity and help cyclones reach their maximum intensity, speed, and movement across the basin on monthly and seasonal time scales. By analyzing observational data and parameters, our goal is to deepen our understanding of TC dynamics and boost our ability to predict them to reduce the human and material damage they cause in the Indian region.

2. Data and Methodology

2.1. Data Used

This study employs satellite and best-track datasets covering the period from 1960 to 2020 to examine atmospheric and oceanic characteristics. Our study specifically examines pre-monsoon (April and May) and post-monsoon (October and November) over the NIO regions (AS and BOB).

The Joint Typhoon Warning Center (JTWC) generated six-hourly TC track data that are utilized in this research [13]. Each best-track file contains information about the centers and intensities of TCs, which are determined based on the highest sustained 10 m wind speed observed over one minute.

The ACE is a quantitative measure of the entire amount of energy discharged by a tropical cyclone throughout its lifespan. The study of ACE offers invaluable insight into the behavior and impacts of tropical cyclones. The ACE index was initially devised and employed by William Gray in 1988 to analyze the damage caused by TC winds and their impact on storm surges, and for the estimation of ACE, wind speeds over 34 knots have been taken into account [14]. The principal objective of the ACE study is to ascertain the destructive capacity of a TC and to calculate the seasonality of such events. A higher ACE value indicates a more destructive cyclone and a more active season. Globally, ACE has shown a decreasing trend as per a recent study from 1991 to 2021 [15]. The wind speed dataset used for the calculation of ACE is obtained from the IBTrACS project [16, 17].

This study also examines many significant parameters that impact the development of cyclones, such as VWS, wind speed, SST, relative vorticity (RV), and relative humidity (RH). The analysis employs ERA5 datasets from the European Centre for Medium-Range Weather Forecasts (ECMWF), which give different time intervals and a geographical resolution of 0.25° × 0.25° [18, 19]. Tropical cyclone heat potential (TCHP) is determined by using potential temperature data obtained and calculated from the Ocean Reanalysis System 5 (ORAS5) monthly dataset, which ECMWF manages.

2.2. Methodology

The calculation of vertical wind shear in the atmosphere follows the methodology described in previous work [20], as shown in Equation (1).

$$VWS = \sqrt{(u_{850} - u_{200})^2 + (v_{850} - v_{200})^2} \quad (1)$$

u_{850} and u_{200} represent the zonal wind components at 850 and 200 hPa pressure levels. Similarly, v_{850} and v_{200} represent the meridional wind components at 850 and 200 hPa pressure levels averaged over the region of interest (60°E–100°E and 5°N–25°N).

The TCHP is calculated using Equation (2),

$$TCHP = \rho Cp \int_0^{D_{26}} [T - 26]\, dz \quad (2)$$

The function T represents the temperature of the considered water layer at depth z, D_{26} indicates the depth at which the isotherms reach a temperature of 26 °C. The specific heat capacity of salt water, denoted as C_p, is taken as 4 $KJkg^{-1}K^{-1}$; ρ is the density of the considered water layer. A greater value of TCHP signifies a more elevated temperature in the ocean, which induces a higher amount of heat available for TC convection due to the transfer of thermal energy between the uppermost layer of the ocean and the atmosphere through evaporation [4].

To compute the ACE, we followed the steps of Waple et al. [21]. This ACE can be used as a climatic indicator for TC seasonal activity and is given by Equation (3).

$$ACE = 10^{-4} \sum\nolimits_{all\ days} v_{max}^2 \quad (3)$$

The ACE is determined by adding up the squared fair value of the estimated maximum sustained winds in knots for the required time when tropical cyclones are present and then converting it to $(m{\cdot}s^{-1})^2$ for simplification. We calculate the ACE for TC that occurs in the NIO region, given that their maximum persistent wind speed should be greater than 17.5 meters per second. This computation includes all days during the months of April, May, October, and November.

Relative vorticity is calculated at the level of 850 hPa by the Equation (4):

$$RV = \frac{\partial v}{\partial x} - \frac{\partial u}{\partial y} \quad (4)$$

where *v* is the meridional wind component, and *u* is the zonal wind component at 850 hPa pressure level averaged over the region of interest (60°E–100°E and 5°N–25°N).

We characterized the TC as per the IMD criteria, which is given below in **Table 1** [22]:

Table 1. Categorization of tropical cyclones as per Indian Meteorological Department (IMD) classification.

SI. No.	Type of Disturbance (Storm)	Associated Maximum Sustained Wind in Knots
1	Low-pressure	Less than 17
2	Depression	17 to 27
3	Deep depression	28 to 33
4	Cyclonic	34 to 47
5	Severe cyclonic	48 to 63
6	Very severe cyclonic	64 to 90
7	Extremely severe cyclonic	91 to119
8	Super cyclonic	120 and above

3. Results and Discussion

We divided the 60 years of the study period into three shorter times for analysis based on several parameters. However, due to the unavailability of ACE data from 1960–1990, we divided the analysis period of ACE into only two different periods for analysis while keeping three time periods for cyclones and other parameters. For ACE, we divided the time into two sub-periods, from 1991–2005 and 2006–2020. The time is divided into three sub-periods for the oceanic and atmospheric parameters: 1960–1990 as Epoch-1,1991–2005 as Epoch-2, and 2006–2020 as Epoch-3, respectively. We selected April and May as pre-monsoon (AM) months and October and November as post-monsoon (ON) months. We did not consider March in our study, as no cyclonic activity was reported during that month. Our study was done using these selected months for all the parameters.

3.1. ACE and Its Variability over the Years

Figure 1 depicts the rate of change in the NIO region over the study period, as determined by ACE trend analysis. The whole energy of the storm that occurred in the NIO basin is accounted for in the ACE for the specified months (AM and ON). Between 1991 and 2005, the ACE trend value showed an annual decreasing trend of $-0.22\ (\mathrm{m \cdot s^{-1}})^2$ with a p-value of 0.192. However, it experienced an increasing trend after 2005, reaching an annual rise of $+0.94\ (\mathrm{m \cdot s^{-1}})^2$ with a p-value of 0.044. This means that the trend of Epoch-3 is more significant than that of Epoch-2. While there may be fluctuations in annual variability, the ACE has exhibited a consistent increasing trend of approximately $+0.26\ (\mathrm{m \cdot s^{-1}})^2$ between 1991 and 2020. In 2019, an ACE above 30 $(\mathrm{m \cdot s^{-1}})^2$ was recorded, the highest value observed during the period. Also, the previous research indicates that the twofold increase in ACE can be primarily attributed to a rise in the frequency and length of very severe cyclonic storms (VSCS) having wind speed above 64 knots[23].

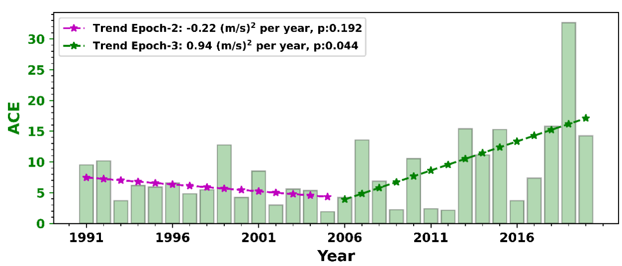

Figure 1. Yearly ACE and trend analysis for 1991–2020.

Figure 2 shows ACE's mean and standard deviation and its spatial distribution across the NIO region from 1991 to 2020. Our study reveals that the vicinity near the Andaman region and the central AS has exhibited more susceptibility to cyclone formation. These specific regions manifest the highest levels of variability across the area, with the central AS showcasing an exceptional standard deviation value exceeding 5 points within designated regions. The distribution of cyclonic activity is notably more widespread in the BoB than in the AS. The eastern coast experiences a more intense cyclonic influence than the western counterpart.

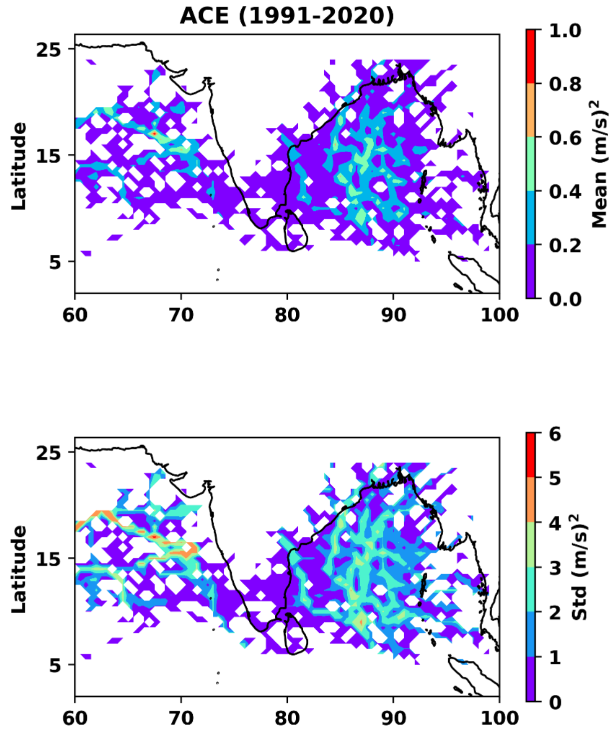

Figure 2. Spatial distribution of ACE over NIO region for 1991–2020.

Despite accounting for fewer than ten percent of the world's TCs, the NIO is significant because it can produce extremely destructive cyclones. This result emphasizes the various paths cyclones might take, highlighting the weaknesses of these coastal regions. On the other hand, the BoB frequently encounters numerous cyclones that reach the coast, particularly affecting Odisha, West Bengal, and the northeastern regions of India. Moreover, substantial cyclonic activity also impacts the Andhra Pradesh and Tamil Nadu states. Subsequently, we conducted a thorough monthly examination of the trajectory and point of impact of the tropical cyclones in the NIO. The findings are presented below.

Figure 3 displays the monthly trajectory of cyclones at three distinct time intervals, as previously delineated for the top four categories. The image depicts the paths of cyclones classified by month; due to a lack of cyclones in March, no track of that month has been included in our study. Hence, our investigation was centered on the pre-monsoon and post-monsoon seasons during three independent time intervals. This study follows the IMD's criteria for the categorization of cyclonic disturbances in the NIO region. Between 1960 and 1990, the eastern coast of India encountered a greater occurrence of cyclones in the period before the monsoon, which then moved towards the southeastern coast in the period after the monsoon. The cyclones that affected the eastern coast were intense and severe storms commonly associated with the development of low-pressure systems in that region.

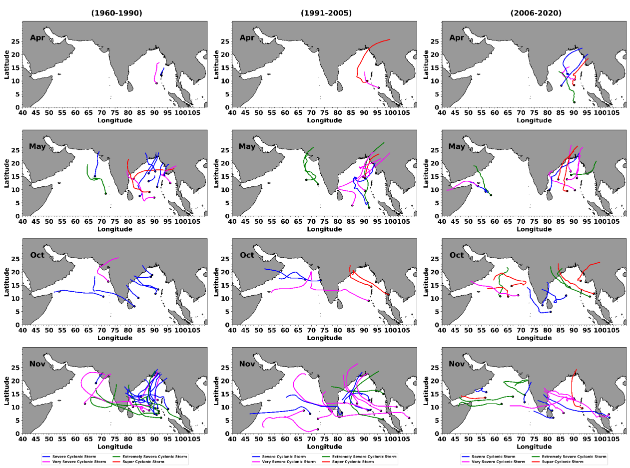

Figure 3. Monthly cyclone track of the top four categories of the cyclone during the different specified periods.

Between 1990 and 2005, northeastern India saw severe cyclones of considerable strength in the pre-monsoon season, with several intense cyclones forming post-monsoon and affecting the southeastern regions. Some cyclones traversed the Indian peninsula, regaining strength and intensifying upon entering the AS.

From 2006 to 2020, similar patterns persisted, with cyclones making landfall both before and after the monsoon seasons, predominantly impacting the southern coast of India, including Andhra Pradesh, Tamil Nadu, the eastern regions near Odisha and West Bengal. While fewer storms reached northeastern India, those that did were powerful cyclones of significant magnitude.

In the NIO basin, approximately 42 cyclonic events (the precise number is unclear due to the unavailability of data) were recorded during 1960–1990, approximately 30 cyclonic activities during 1991–2005, and approximately 41 cyclonic activities during 2006–2020.

3.2. Spatial Distribution and Influence of Various Atmospheric and Oceanic Parameters

High SST, VWS, Tropical Cyclone Heat Potential (TCHP), Wind, Relative Vorticity (RV), and Specific Humidity (SH) are all elements required for cyclogenesis and also control the intensity and movement of the cyclone along its path [3, 4, 24–26]. The NIO basin is a good place for cyclone development since all the conditions exist. To determine if these factors meet the requirements for cyclogenesis, we investigate the monthly variation of these parameters over three-time scales from 1960 to 2020 on a selected monthly basis.

3.2.1. Variations of Wind Climatology for Different Epochs

Seasonal variance of wind during different Epochs is shown in **Figure 4**. Wind is a vital component in the process of cyclogenesis. In April, we observed that the wind speeds were consistently below 2 $(\mathrm{m{\cdot}s^{-1}})^2$. In May, the wind variance remains rather high, reaching around 4.5 $(\mathrm{m{\cdot}s^{-1}})^2$. In some regions, it may surpass this number, particularly in the pre-monsoon season. During the post-monsoon season, wind speed variance fluctuates between 4–6 $(\mathrm{m{\cdot}s^{-1}})^2$, which is observed in both months in the zones of cyclogenesis in southern India and the Andaman region. The wind values in central AS were higher in May but lower in April during Epoch-1. However, the area near the equator has an increase in value after the monsoon season. Epoch-2 had comparable monthly trends; however, Epoch-3 experienced a decline in values throughout the pre-monsoon season. During the pre-monsoon season, there is minimal wind variability, with fluctuations of less than 1 $(\mathrm{m{\cdot}s^{-1}})^2$. Similar to the pre-monsoon season, November has a comparatively lower value ranging from 1.5 to 2.5 $(\mathrm{m{\cdot}s^{-1}})^2$, whereas October has a considerably higher value ranging from 4 to 6 $(\mathrm{m{\cdot}s^{-1}})^2$ and above over some parts. The BoB region shows higher variation than the AS region in all the periods in almost all of the months except in May during Epoch-2. Typically, the months of May, October, and November see higher wind speeds during the periods before and after the monsoon season compared to April. Cyclogenesis needs a greater wind value, and the post-monsoon season offers largely ideal conditions for the development of cyclones of higher categories.

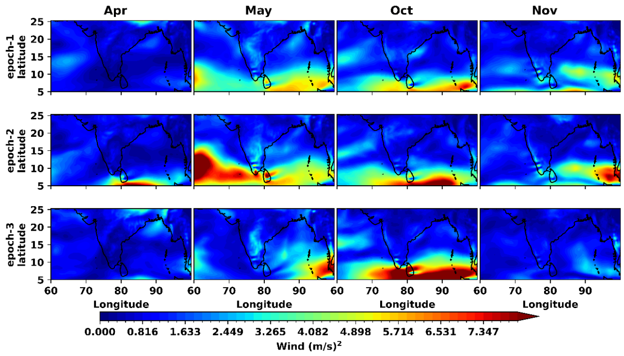

Figure 4. Monthly variance of wind value from 1960 to 2020 for different epochs.

3.2.2. Variations of Specific Humidity Climatology for Different Epochs

The seasonal variance of SH during different Epochs is shown in **Figure 5**. As previous studies show, humidity helps intensify TCs and their movement. An increase in the humidity at a particular place may favor cyclogenesis if other environmental conditions are satisfied. When we look at specific humidity, the months of April, May, and November exhibit larger variances in their values, ranging from 1.75×10^{-6} to 2.2×10^{-6} $(\mathrm{kg\cdot kg^{-1}})^2$. But during Epoch-2, the month of May exhibits more than 2.5×10^{-6} $(\mathrm{kg\cdot kg^{-1}})^2$ variance. Furthermore, substantial fluctuations in SH levels are observed along the western coast and in the northern BoB region throughout the entire post-monsoon season in November in most of the epochs. This suggests that the region contains a substantial amount of SH, which is required for the formation of cyclones. The elevated levels of SH are strongly associated with the strengthening of TCs and show more number of extreme cyclones during Epoch-3, although the numbers are less. During Epoch-2, more higher category cyclones have been recorded during post-monsoon season. During the pre-monsoon period, a considerable degree of variability in SH levels was observed in the central AS and the southwestern coast of India. The MDR in AS has exhibited a considerable degree of variability, which could potentially impact the rapid intensification of cyclones.

3.2.3. Variations of Relative Vorticity Climatology for Different Epochs

Seasonal variance of RV during different Epochs is shown in **Figure 6**. The curvature of an airflow is measured by its vorticity. Cyclone formation is encouraged by a favorable vorticity environment. The main environmental component influencing TC intensification is vorticity. Positive RV readings result in rapid ascent [27]. RV shows a very small change in its variance, but the southern Indian peninsula and northeastern part of India show the maxmium variance value for all the periods from 1960 to 2020. For TCs to develop and intensify, momentum, mass, and water vapor must be continuously imported. Assuming all other conditions are suitable and stay stable, the formation of TCs might be closely linked to the strength of the low-level tropospheric RV [28]. The RV values exhibited reduced variability throughout the ocean in both the pre-monsoon and post-monsoon periods. However, during Epoch-3, there was an increase in the value of the variable, particularly over the ocean region where MDR is situated, having a value of more than $1.02 \times 10^{-10}\ \mathrm{s}^{-1}$, compared to earlier periods. This rise favored the formation of cyclones.

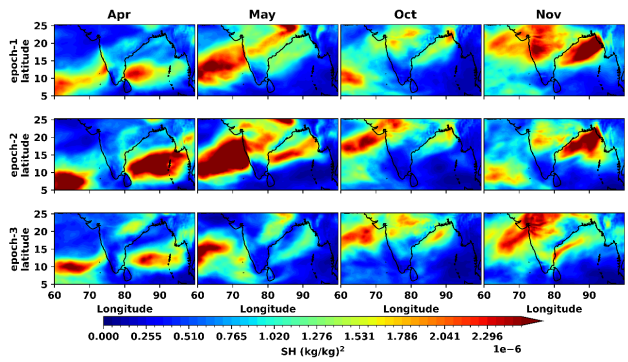

Figure 5. Monthly variance of specific humidity from 1960 to 2020 for different epochs.

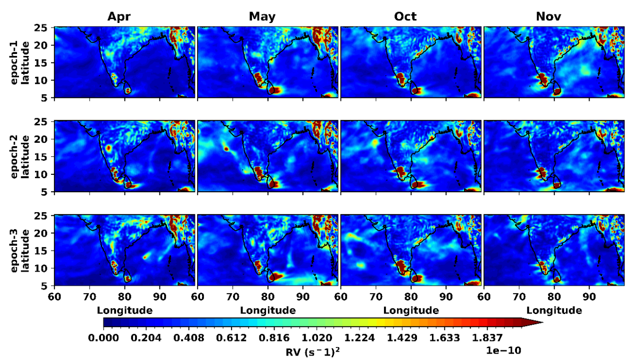

Figure 6. Monthly variance of relative vorticity from 1960 to 2020 for different epochs.

3.2.4. Variations of Sea Surface Temperature Climatology for Different Epochs

Seasonal variance of SST during different Epochs is shown in **Figure 7**. The SST is the main component that affects the TC formation, especially in the NIO, because of its proximity near to the equator and the surrounding physical characteristics. The BoB has more SST variations in comparison to the AS. Between 1960 and 2020, the fluctuation in SST has usually been more during the pre-monsoon season than during the post-monsoon season. During the months following the monsoon season, the SST varies between 0.2 and 0.3 °C². In the period before the monsoon season, the normal range of SST fluctuations is between 0.1 and 0.2 °C².

During Epoch-1, notable SST variations were recorded along the western coast of India near the Gujarat region during April, October, and November months, surpassing 0.25 °C². During the post-monsoon season, significant variability was seen along the west coast of India and central AS compared to the BoB. In contrast, Epoch-2 exhibited similar or higher values in some places than in the previous epoch during the post-monsoon season. During Epoch-3, the pre-monsoon season in the BoB saw a higher range of SST fluctuation, ranging from 0.24 to 0.3 °C² near the Andaman region. If we look at **Figure 3**, it may be concluded that higher SST variance in April over MDR in BoB is one of the major causes that enhance the TC activity in the BoB region compared to the previous two epochs. The post-monsoon season shows lesser changes, ranging from 0.07 to 0.12 °C² over the region. November shows lower SST variance, which results in lower TC activity during that period.

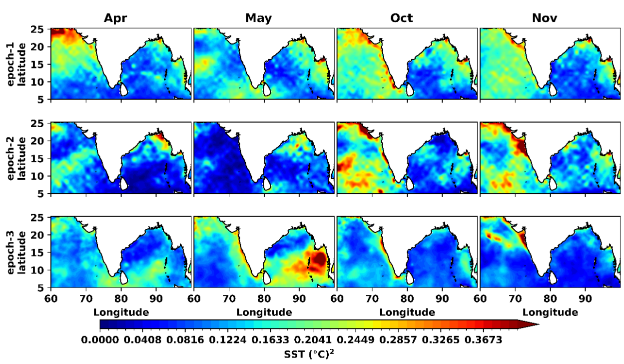

Figure 7. Monthly variance of sea surface temperature from 1960 to 2020 for different epochs.

3.2.5. Variations of VWS Climatology for Different Epochs

Seasonal variance of VWS during different epochs is shown in **Figure 8**. The presence of VWS in the atmosphere has a good influence on the structure and intensity of TC [29, 30]. Increased VWS negatively impacts cyclone formation, as demonstrated in the study of Kerns and Chen [31]. However, there is evidence [32–34] that suggests mild to moderate VWS is advantageous for the formation of cyclones. Prior research has demonstrated that a reduction in VWS benefits the development of cyclones.

Across all epochs (from 1960 to 2020), there was a notable variation in May and October, with a prevailing occurrence of high VWS over a few regions near MDR. Consequently, this may result in a deficiency of cyclogenesis over a few locations during that particular month. All prior pre-monsoon and post-monsoon seasons have demonstrated favorable low VWS during all epochs over the MDR. During all months over the MDR, where the majority of cyclogenesis in both the AS and BoB occurs, the VWS variance is observed to be weak, with a value of less than 5 (m·s–²). Higher variance in VWS was observed across all three time periods, from 1960 to 2020, during October near the equatorial region. In the pre-monsoon season, April exhibits slightly higher VWS variance if we look into the MDR in AS than in May; this may be the reason for less cyclonic activity during this time, while the region proximate to the MDR in BoB displays a higher value in May. Additionally, elevated VWS variance is evident over the Deccan Plateau of India and the southern Indian region in October.

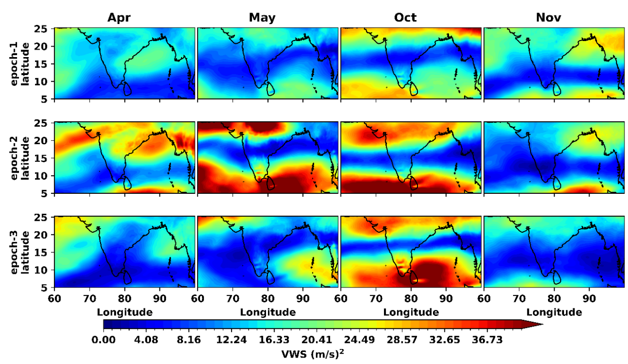

Figure 8. Monthly variance of vertical wind shear from 1960 to 2020 for different epochs.

3.2.6. Variations of TCHP Climatology for Different Epochs

Seasonal variance of TCHP during different epochs is shown in **Figure 9**. This measure is calculated worldwide using upper ocean vertical temperature profiles acquired from altimeters [4]. High TCHP readings correlate strongly with TC intensification [35]. The lesser variance was observed during the first two epochs, with a range of

200-−250 $(\mathrm{KJ}\cdot\mathrm{cm}^{-2})^2$ in April, and in contrast, the third period exhibited a higher variance, with a range of 430−530 $(\mathrm{KJ}\cdot\mathrm{cm}^{-2})^2$ in the AS region. In May, the first two epochs exhibited a lesser degree of variance in comparison to the third period, during which a variance exceeding 450 $(\mathrm{KJ}\cdot\mathrm{cm}^{-2})^2$ was observed across numerous locations in both basins. The Central BoB demonstrates a higher degree of variation, with values ranging between 300 and 400 $(\mathrm{KJ}\cdot\mathrm{cm}^{-2})^2$.

Meanwhile, during the post-monsoon season, a markedly elevated TCHP variance was observed in October and November, reaching over 500 $(\mathrm{KJ}\cdot\mathrm{cm}^{-2})^2$ in the vicinity of the northeastern coast of India. In contrast, the three post-monsoon season epochs exhibited a markedly reduced variance value in comparison to the pre-monsoon season over the MDR. SST and TCHP are correlated and key factors for cyclogenesis over that region.

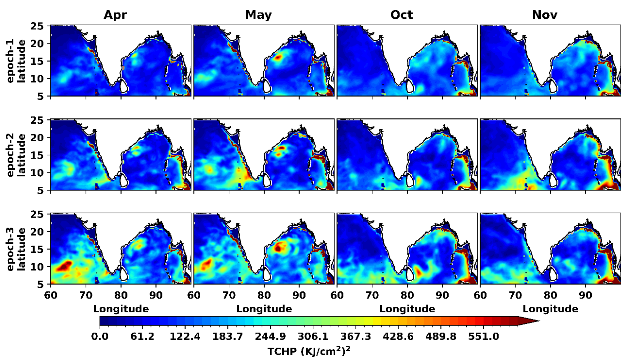

Figure 9. Monthly variance of tropical cyclone heat potential mean from 1960 to 2020 for different epochs.

4. Conclusions

The study period of 1960–2020 is divided into three subperiods to analyze the long-term variations in the atmospheric and oceanic parameters that influence cyclonic activity. The ACE index demonstrates a negative trend during Epoch-1 but a positive trend during Epoch-2, with a higher level of statistical significance. Following 2013, higher values in ACE can be observed, with the highest recorded value occurring in 2019 at over 30 $(\mathrm{m}\cdot\mathrm{s}^{-1})^2$. The ACE was most prevalent in the BoB region in comparison to AS, exhibiting a lesser degree of deviation from its mean value. The majority of cyclones that occurred in the BoB region were of a higher category than those that occurred in the AS region. During the pre-monsoon period, the majority of cyclones make landfall in the northeastern region of India, yet make landfall in the southeastern region of India during the post-monsoon season. A greater number of extreme cyclones were recorded during the post-monsoon period.

The BoB is renowned for its proclivity to spawn higher-category cyclones, particularly during the monsoon season. Upon thorough examination of the parameters, the phenomenon becomes evident. It experiences a greater frequency of cyclonic disturbances. From 1990 to 2020, there has been a consistent increase in the intensity of tropical cyclones (severe cyclonic storms and stronger) in the NIO, which is different from the previous three decades (1960–1990). The findings indicate that higher SST, RH, RV, SH, wind, and TCHP values are identified as significant contributors to the ACE essential for cyclone genesis and intensification.

Furthermore, the combination of elevated SST and RH, along with low VWS, creates optimal atmospheric conditions for sustaining cyclones at their maximum intensity, and these variables show maximum variability across the basins. Conversely, the incidence of tropical cyclones over the BoB has exhibited a decline over the same period. The higher category cyclones majorly occurred in the post-monsoon season, which contributes to higher ACE values as the higher the category, the higher the ACE related to it. During epoch 3, there is a notable pattern of variances across different basins. Specifically, BoB exhibits a lower SH variance, particularly in November and May, and a lower SST variance in October and November.

Additionally, the variance of VWS over the MDR is reduced in both basins during May and November. Overall, there is a generally higher variance of TCHP across all basins during Epoch-3. The BoB experienced reduced events in the month of November as well as in the month of May, which may be due to decreased SH levels. However, lower VWS and higher SST/ TCHP may have the reason of increased extreme/ super TC events in the month of May. A notable shift in SH between the BoB and AS during epoch 3 may explain the high number of super cyclonic storms.

Overall, the study reveals significant fluctuations in TC features and severity in May and November, with October and November showing the most pronounced alterations. These findings highlight the interplay between regional thermodynamic and dynamic elements influencing TC activity in the NIO. This can be improved by understanding the parameters and their correlation with TC activity and facilitating the prediction of TCs using diverse models and machine learning methodologies.

Author contributions

Conceptualization, methodology, software, validation, formal analysis, investigation, resources, data curation, writing-original drafts, and visualization; A.K.S.; conceptualization, investigation, writing—review, editing, and supervision, A.C.

Funding

There is no funding for this work.

Institutional Review Board Statement

Not applicable.

Informed Consent Statement

Not applicable.

Data Availability Statement

The data used in this study are publicly available. The authors will be happy to share the data used in the manuscript upon request.

Acknowledgments

We express our gratitude to the Indian Institute of Technology Kharagpur for providing the necessary facilities to carry out this research work and gratefully acknowledge MHRD for giving a research fellowship. The Graphics were created using Python 3.9. We are greatful to the anonymous reviewers for the constructive comments and suggestions that help to improve the quality and standard of the manuscript.

Conflict of Interest

The authors declare no conflict of interest in this study. The ethical standards were considered in the study.

References

[1] Singh, V.K., Roxy, M.K., 2022. A review of ocean-atmosphere interactions during tropical cyclones in the north Indian Ocean. Earth-Science Reviews. 226, 103967.

[2] Lin, I.I., Chen, C.H., Pun, I.F., et al., 2009. Warm ocean anomaly, air sea fluxes, and the rapid intensification of tropical cyclone Nargis (2008). Geophysical Research Letters. 36(3).

[3] Gray, W.M., 1968. Global view of the origin of tropical disturbances and storms. Monthly Weather Review. 96(10), 669–700.

[4] Leipper, D.F., Volgenau, D., 1972. Hurricane heat potential of the Gulf of Mexico. Journal of Physical Oceanography. 2(3), 218–224.

[5] Lead, T., 2013. National Cyclone Risk Mitigation Project (NCRMP). V22, March 2013.

[6] Geetha, B., Balachandran, S., 2014. Decadal variations in translational speed of cyclonic disturbances over North Indian Ocean. Mausam. 65(1), 115–118.

[7] Priya, P., Pattnaik, S., Trivedi, D., 2022. Characteristics of the tropical cyclones over the North Indian Ocean Basins from the long-term datasets. Meteorology and Atmospheric Physics. 134(4), 65.

[8] Deshpande, M., Singh, V.K., Ganadhi, M.K., et al., 2021. Changing status of tropical cyclones over the north Indian Ocean. Climate Dynamics. 57, 3545–3567.

[9] Kabir, R., Ritchie, E.A., Stark, C., 2022. Tropical cyclone exposure in the North Indian Ocean. Atmosphere. 13(9), 1421.

[10] Pfleiderer, P., Schleussner, C.F., Geiger, T., et al., 2020. Robust predictors for seasonal Atlantic hurricane activity identified with causal effect networks. Weather and Climate Dynamics. 1(2), 313–324.

[11] Camargo, S.J., Sobel, A.H., 2005. Western North Pacific tropical cyclone intensity and ENSO. Journal of Climate. 18(15), 2996–3006.

[12] Knutson, T.R., Chung, M.V., Vecchi, G., et al., 2021. Climate Change is Probably Increasing the Intensity of Tropical Cyclones. In: Critical Issues in Climate Change Science. DOI: https://doi.org/10.5281/zenodo.4570334

[13] Chu, J.H., Sampson, C.R., Levine, A.S., et al., 2002. The Joint Typhoon Warning Center Tropical Cyclone Best-Tracks, 1945–2000. Ref. NRL/MR/7540-02.

[14] Gray, W.M., 1988. Forecast of Atlantic Seasonal Hurricane Activity for 1988. Report number, 26 May 1988.

[15] Klotzbach, P.J., Wood, K.M., Schreck III, C.J., et al., 2022. Trends in global tropical cyclone activity: 1990–2021. Geophysical Research Letters. 49(6), e2021GL095774.

[16] Knapp, K.R., Kruk, M.C., Levinson, D.H., et al., 2010. The international best track archive for climate stew-

ardship (IBTrACS) unifying tropical cyclone data. Bulletin of the American Meteorological Society. 91(3), 363–376.

[17] Knapp, K.R., Diamond, H.J., Kossin, J.P., et al., 2018. International best track archive for climate stewardship (IBTrACS) project, version 4. NOAA National Centers for Environmental Information, 10.

[18] Hersbach, H., Bell, B., Berrisford, P., et al., 2018a. ERA5 hourly data on pressure levels from 1979 to present. Copernicus Climate Change Service (C3s) Climate Data Store (Cds), 10.

[19] Hersbach, H., Bell, B., Berrisford, P., et al., 2018b. ERA5 hourly data on single levels from 1979 to present. Copernicus Climate Change Service (C3S) Climate Data Store (CDS).

[20] Evan, A.T., Camargo, S.J., 2011. A climatology of Arabian Sea cyclonic storms. Journal of Climate. 24, 140–158.

[21] Waple, A.M., Lawrimore, J.H., Halpert, M.S., et al., 2002. Climate assessment for 2001. Bulletin of the American Meteorological Society. 83(6), S1–S62.

[22] IMD, 2013. Cyclone Warning in India: Standard Operation Procedure. SOP No. 10/2013, 200p.

[23] Balaji, M., Chakraborty, A., Mandal, M., 2018. Changes in tropical cyclone activity in north Indian Ocean during satellite era (1981–2014). International Journal of Climatology. 38(6), 2819–2837.

[24] Kumar, B., Chakraborty, A., 2011. Movement of seasonal eddies and its relation with cyclonic heat potential and cyclogenesis points in the Bay of Bengal. Natural Hazards. 59, 1671–1689.

[25] Kumar, A., Chakraborty, A., Sadhukhan, B., 2023. Sequential occurrence and development of three tropical cyclones in the Bay of Bengal in 2013. Dynamics of Atmospheres and Oceans. 102, 101363.

[26] Roy Chowdhury, R., Prasanna Kumar, S., Narvekar, J., et al., 2020. Back-to-back occurrence of tropical cyclones in the Arabian Sea during October–November 2015: Causes and responses. Journal of Geophysical Research: Oceans. 125(6), e2019JC015836.

[27] Reed, R.J., Recker, E.E., 1971. Structure and properties of synoptic-scale wave disturbances in the equatorial western Pacific. Journal of the Atmospheric Sciences. 28(7), 1117–1133.

[28] Gray, W.M., 1975. Tropical cyclone genesis [PhD thesis]. Fort Collins, CO: Colorado State University. p. 234.

[29] DeMaria, M., 1996. The effect of vertical shear on tropical cyclone intensity change. Journal of Atmospheric Sciences. 53(14), 2076–2088.

[30] Zehr, R.M., 2003. Environmental vertical wind shear with Hurricane Bertha (1996). Weather and Forecasting. 18(2), 345–356.

[31] Kerns, B.W., Chen, S.S., 2013. Cloud clusters and tropical cyclogenesis: Developing and nondeveloping systems and their large-scale environment. Monthly Weather Review. 141(1), 192–210.

[32] Bracken, W.E., Bosart, L.F., 2000. The role of synoptic-scale flow during tropical cyclogenesis over the North Atlantic Ocean. Monthly weather review. 128(2), 353–376.

[33] Nolan, D.S., McGauley, M.G., 2012. Tropical cyclogenesis in wind shear: Climatological relationships and physical processes. Cyclones: Formation, Triggers, and Control. 1, 34.

[34] Reasor, P.D., Montgomery, M.T., 2001. Three-dimensional alignment and corotation of weak, TC-like vortices via linear vortex Rossby waves. Journal of the Atmospheric Sciences. 58(16), 2306–2330.

[35] Mainelli, M., DeMaria, M., Shay, L.K., et al., 2008. Application of oceanic heat content estimation to operational forecasting of recent Atlantic category 5 hurricanes. Weather and Forecasting. 23(1), 3–16.